Journal of Sound and Vibration (2001) **246**(2), 265–280
doi:10.1006/jsvi.2001.3636, available online at http://www.idealibrary.com on IDEAL®

LOSS FACTOR PEAK OF VISCOELASTIC MATERIALS: MAGNITUDE TO WIDTH RELATIONS

T. PRITZ

Acoustics Laboratory, Szikkti Labs, 1301 *Budapest, Pf.* 81, *Hungary*

(*Received* 17 *August* 2000, *and in final form* 10 *January* 2001)

The loss factor of viscoelastic materials as a function of frequency has at least one peak. The relation between the magnitude and width of the loss factor peak is investigated in this paper by means of the fractional derivative Zener model with special reference to polymeric materials used for sound and vibration damping. It is shown that the magnitude and width are interrelated through the dispersion of dynamic modulus and the rate of frequency variation of loss factor. Moreover, it is proved that the relation between the magnitude and width of the loss factor peak is not unequivocal; either proportionality or inverse proportionality may exist between them. The important consequence of prediction on the proportionality is that, in contrast to the common belief concerning polymers, it is physically possible to increase the loss factor while simultaneously broadening the peak. The validity of model predictions is discussed and it is proved that the predictions are of a general nature, because they obey fundamental physical principles. Experimental data supporting the theoretical predictions are presented.

1. INTRODUCTION

The passive methods of sound and vibration damping require materials having high energy absorbing capacity. Organic polymers, especially the elastomers, are the most effective and widely used for this purpose. Some of the more important polymeric damping materials include natural and synthetic rubbers, polyurethanes, acrylics, etc., to mention only a few. In addition, the rigid plastics, polymer composites and certain glasses have higher damping than the common stiff structural materials. The polymeric materials are frequently referred to as viscoelastic ones; however, the phenomena of viscoelastic behaviour are more or less characteristics of all real solid materials [1].

One of the more notable phenomena of viscoelastic behaviour is the frequency dependence of the loss factor used to characterize the damping in materials. It is known that the loss factor of a viscoelastic material passes through at least one peak as a function of frequency [2–4]. The peak may be either high or low, narrow or broad, but its existence is typical of real solid materials [5]. The location and magnitude of the loss factor peak are of primary interest in damping applications, but the peak width has special importance as well, since the usual aim in damping applications is to realize high damping over as wide a frequency range as possible.

Many efforts have been made to increase the efficiency (i.e., both the magnitude and width of the loss factor peak) of damping materials, especially the polymeric ones, by tailoring their structure, adding fillers, etc. Unfortunately, it has been observed for many polymers, such as rubbers [6, 7] and polyurethanes [8–10], that the peak magnitude decreases if the width is increased and vice versa. As a result of these observations, a belief

0022-460X/01/370265 + 16 $35.00/0

that the magnitude and width of the loss factor peak of polymers are inversely related has generally been accepted. Notwithstanding this, there are published experimental results that are inconsistent with this belief. Specifically, the loss factor of some rubbery materials may increase while simultaneously the peak broadens due to special fillers [7, 11]. More recently, research on interpenetrating network polymers has revealed that the loss factor can be increased without decreasing the peak width, and might even slightly increase it [12]. Furthermore, some experimental data show that the peak width is about the same for some polymer based damping materials, while their loss factors are dissimilar. Such data will be presented in the paper. These experimental results raise doubts that the inverse relation would be a general law for polymeric materials.

The theoretical studies of the relation between the magnitude and width of the loss factor peak are contradictory as well. The problem has been investigated by means of viscoelastic models and the inverse relation has been found [13–15]. Conversely, a numerical study of one of the models used to prove the inverse relation has drawn attention to the fact that the peak width can be increased without decreasing the loss factor maximum [16].

Therefore, the question rightly arises about the relation that may exist between the magnitude and width of the loss factor peak. Is the inverse relation generally valid for polymers or only for some of them? The question may be put in general terms, concerning the loss factor peak of other solid materials. Finding the right answer to this question may help to clear up a basic problem of damping material research; whether or not there is a fundamental barrier to increasing the loss factor while simultaneously broadening the peak width.

The aim of this paper is to answer the above questions. The fractional derivative Zener model, which is able to describe the linear viscoelastic behaviour of polymers and other solid materials over a wide frequency range [16–21] will be used for this purpose. This model can be regarded as a modification of the conventional Zener model, also known as the standard linear solid, by introducing the fractional order time derivatives into the model constitutive equation [17]. The limits of the model predictions will be discussed and it will be shown that the predictions are of a general nature, because they obey fundamental physical principles. Experimental data will be presented and compared with the theoretical predictions.

2. THEORY

2.1. DYNAMIC PROPERTIES AS FUNCTIONS OF FREQUENCY

The linear damping properties of solid materials are usually characterized through the complex modulus concept. Of the complex moduli, the complex shear modulus $\bar{G}$, playing a fundamental role in materials science and engineering, is used in this paper. The general definition of $\bar{G}$ is

$$\bar{G}(\mathrm{j}\omega) = \frac{\tilde{\sigma}(\mathrm{j}\omega)}{\tilde{\varepsilon}(\mathrm{j}\omega)} = G_d(\omega) + \mathrm{j}G_l(\omega) = G_d(\omega)[1 + \mathrm{j}\eta(\omega)], \tag{1}$$

where $\tilde{\sigma}(\mathrm{j}\omega)$ and $\tilde{\varepsilon}(\mathrm{j}\omega)$ are the Fourier transforms of the stress- and strain-time histories respectively, $\mathrm{j} = \sqrt{-1}$ is the imaginary unit, $\omega = 2\pi f$. f is the frequency in Hz, G_d is the dynamic shear modulus, G_l is the shear loss modulus and η is the loss factor,

$$\eta(\omega) = G_l(\omega)/G_d(\omega). \tag{2}$$

The complex modulus of elasticity describes the material behaviour in the frequency domain, and all its components depend on the frequency. It is known from many experiments that the dynamic modulus of viscoelastic materials increases with increasing frequency, and the loss functions pass through one or more maxima [2–4]. It has been proved recently that these characters of frequency dependences and the existence of at least one loss maximum are typical of real solid materials regardless of the mechanism of damping [5]. The frequency variations of dynamic modulus, loss modulus and loss factor are illustrated in Figure 1, with the assumption that the loss peak is symmetrical with respect to logarithmic frequency. (The case of asymmetrical loss peak and the related problems will be discussed in section 2.2) The quantitative characteristics of these frequency functions are: the static modulus of elasticity G_0, the high frequency limit value of dynamic modulus G_∞, the maximum slope of $\log G_d(\omega)$ versus $\log \omega$ curve, the maximum values (G_m, η_m) and the relevant frequencies (ω_l, ω_η) of the loss functions, the slope of increase and decrease of the loss functions measured far from their peak. Moreover the half-width of loss peaks defined as

$$\Delta\omega = \omega_2 - \omega_1, \tag{3a}$$

where ω_1 and ω_2 are the frequencies at the half value of the peak maximum. For practical purposes, the difference between the logarithmic values of ω_1 and ω_2 will be used in the paper to characterize numerically the half-width, and it is denoted by W:

$$W = \log(\omega_2/\omega_1). \tag{3b}$$

Note that although the quantitative characteristics are dependent on the material in question, some of them are interrelated. In particular, the magnitude of the loss factor peak is known to be related to the maximum slope of the $\log G_d(\omega)$ versus $\log \omega$ curve through the dispersion relations [5]. Furthermore, as can be seen in Figure 1, this slope is related to the difference between G_∞ and G_0, and to the half-width. In addition, it is clear that the half-width is related to the slope of frequency variation of the loss factor measured far from the peak. All these suggest that the loss factor maximum, the width, the slope of frequency variation of the loss factor and the modulus difference are interrelated. The experimental

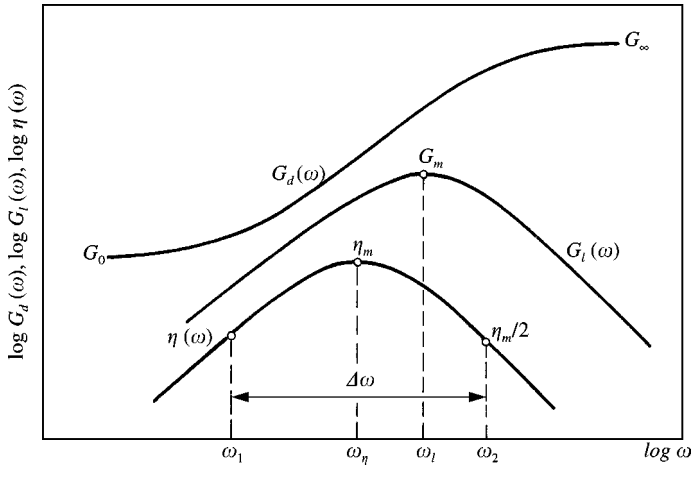

Figure 1. Typical frequency dependences of the dynamic shear modulus, loss modulus and loss factor of viscoelastic materials.

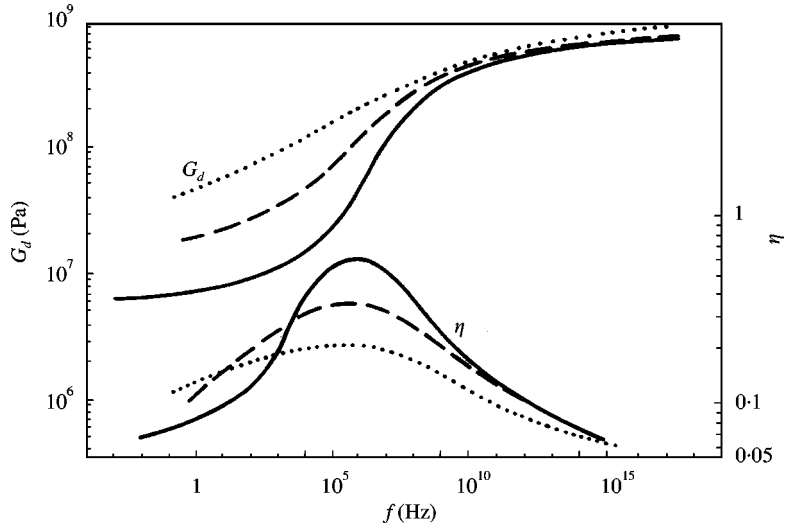

Figure 2. It has been observed for some polymers that the loss factor maximum decreases while simultaneously the peak broadens. The frequency curves relate to polyurethanes samples, and are from Duffy *et al.* [9].

observation concerning some polymers, that the loss factor maximum decreases while simultaneously the peak broadens, is illustrated as an example in Figure 2 for polyurethane samples [9]. Notwithstanding this, it is not clear from the above train of thought why it should be exclusively so.

2.2. MAGNITUDE TO WIDTH RELATIONS

The analytical investigation of the relation between the maximum and the width of the loss factor peak requires a mathematical description of the frequency variations of the dynamic properties. The fractional derivative Zener model [21], also known as the four-parameter fractional derivative model [16, 20], has been shown to be an effective tool to describe frequency variations such as those illustrated in Figure 1. This model has a sound theoretical basis and it has successfully been used to fit experimental data for a wide variety of materials [16–20]. These facts show promise for finding general relations between the loss factor maximum and the width by means of this model.

The behaviour of the fractional derivative Zener model, referred to in short as the fractional Zener model, was studied in detail in a previous work by the author [16]. The most important relationships needed for this investigation were derived in that work, but are repeated here for the sake of clarity.

The complex modulus describing the frequency dependences of dynamic properties for this model is derivable from the model constitutive equation, which defines the stress to strain relationship in the time domain as

$$\sigma(t) + \tau_r^\alpha D^\alpha[\sigma(t)] = G_0\varepsilon(t) + G_\infty \tau_r^\alpha D^\alpha[\varepsilon(t)], \tag{4}$$

where t is the time, τ_r is the relaxation time, $0 < \alpha < 1$, and D^α denotes the operator of fractional derivation of αth order defined as [16]

$$D^\alpha[\sigma(t)] = \frac{1}{\Gamma(1-\alpha)} \frac{\mathrm{d}}{\mathrm{d}t} \int_0^t \frac{\sigma(\tau)}{(t-\tau)^\alpha} \mathrm{d}\tau, \tag{5}$$

in which Γ is the gamma function, and τ is a dummy variable. Note that equation (4) gives the constitutive equation for the conventional Zener model if $\alpha = 1$. The transformation of equation (4) into the frequency domain results in the complex modulus for the fractional Zener model. It is easy to perform the transformation, bearing in mind that the Fourier transform of the operator D^α yields $(j\omega)^\alpha$, so that the complex modulus is

$$\bar{G}(j\omega) = \frac{G_0 + G_\infty (j\omega\tau_r)^\alpha}{1 + (j\omega\tau_r)^\alpha}. \tag{6a}$$

This equation can be re-arranged in the form:

$$\frac{\bar{G}(j\omega) - G_\infty}{G_0 - G_\infty} = \frac{1}{1 + (j\omega\tau_r)^\alpha}, \tag{6b}$$

which is often referred to as the Cole–Cole equation, after the authors who introduced formally the same equation to fit experimental data of complex dielectric functions of polymers [22].

The components of the complex shear modulus are given in a normalized form for the sake of convenience:

$$\frac{G_d(\omega)}{G_0} = \frac{1 + (c+1)\cos(\alpha\pi/2)\omega_n^\alpha + c\omega_n^{2\alpha}}{1 + 2\cos(\alpha\pi/2)\omega_n^\alpha + \omega_n^{2\alpha}}, \tag{7}$$

$$\frac{G_l(\omega)}{G_0} = \frac{(c-1)\sin(\alpha\pi/2)\omega_n^\alpha}{1 + 2\cos(\alpha\pi/2)\omega_n^\alpha + \omega_n^{2\alpha}}, \tag{8}$$

$$\eta(\omega) = \frac{(c-1)\sin(\alpha\pi/2)\omega_n^\alpha}{1 + (c+1)\cos(\alpha\pi/2)\omega_n^\alpha + c\omega_n^{2\alpha}}, \tag{9}$$

where

$$c = G_\infty / G_0. \tag{10}$$

The symbol c characterizes the dispersion of the dynamic modulus, and ω_n is the normalized frequency:

$$\omega_n = \omega\tau_r. \tag{11}$$

The variations of the normalized dynamic modulus and the loss factor are illustrated as examples in Figures 3 and 4 as functions of normalized frequency, with the values of $G_\infty/G_0 = 10^2$ and $\alpha = 1{\cdot}0$, $0{\cdot}7$, $0{\cdot}5$ (Figure 3), and for $\alpha = 0{\cdot}7$ and $G_\infty/G_0 = 10$, 10^2, 10^3 (Figure 4). It can be seen in both figures, that α is the slope of $\log\eta$ versus $\log\omega$ curve measured far from the peak maximum. In addition, it can be seen in Figure 3, that the larger the loss factor maximum, the smaller the peak width. This is in accord with the belief that the magnitude and width of the loss factor peak are inversely related for polymeric materials. In contradiction to this, Figure 4 shows that the loss factor maximum increases while simultaneously the peak broadens. This latter fact seems to disprove that the inverse relation would be generally valid.

In order to find the reason for the above contradiction, the maximum value and the half-width of the loss factor peak are derived. For the sake of completeness, these quantities are also determined for the loss modulus peak. It can be proved by a well-known method

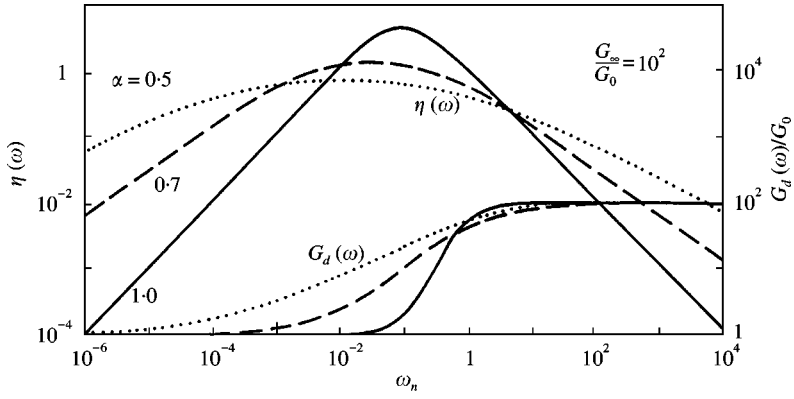

Figure 3. Frequency variations of the dynamic modulus and loss factor calculated by the fractional Zener model, with the assumption that the modulus dispersion is constant; $G_\infty/G_0 = 10^2$.

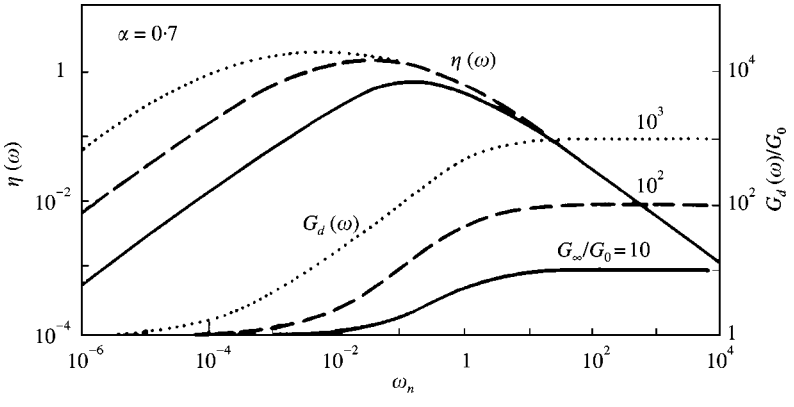

Figure 4. Frequency variations of the dynamic modulus and loss factor calculated by the fractional Zener model, with the assumption that the αth order of fractional derivative is constant.

that the maximum of the loss modulus occurs at $\omega_n = 1$, and the maximum of the loss factor is at a normalized frequency of

$$\omega_n = 1/\sqrt[2\alpha]{c}\,. \tag{12}$$

The maximum of the loss modulus normalized to M_0 is

$$\frac{M_m}{M_0} = \frac{c-1}{2}\,\frac{\sin(\alpha\pi/2)}{1+\cos(\alpha\pi/2)} \tag{13}$$

and the maximum of the loss factor is

$$\eta_m = \frac{c-1}{2\sqrt{c}}\,\frac{\sin(\alpha\pi/2)}{1+[(c+1)/2\sqrt{c}]\cos(\alpha\pi/2)}. \tag{14}$$

The half-widths are

$$W_l = \log\left(\frac{\omega_2}{\omega_1}\right)_l = \frac{1}{\alpha}\log\frac{A+\sqrt{A^2-1}}{A-\sqrt{A^2-1}} \tag{15}$$

and

$$W_\eta = \log\left(\frac{\omega_2}{\omega_1}\right)_\eta = \frac{1}{\alpha}\log\frac{B+\sqrt{B^2-1}}{B-\sqrt{B^2-1}}, \tag{16}$$

where the subscripts l and η refer to the loss modulus and loss factor, respectively, and

$$A = 2 + \cos(\alpha\pi/2) \tag{17}$$

and

$$B = 4\sqrt{c} + (c+1)\cos(\alpha\pi/2). \tag{18}$$

It is clear from equation (15) that the half-width of the loss modulus peak is dependent on α only. The values of W_l are plotted in Figure 5 versus α. It is seen that the half-width of the loss modulus peak increases by decreasing α, as expected. In contrast to the loss modulus, the width of loss factor peak is related to the modulus dispersion G_∞/G_0 as well as α. One can see, in Figure 5, where the values of W_η are plotted versus α for $G_\infty/G_0 = 10$, 10^2, 10^3 and 10^4, that the larger the modulus dispersion, the broader the loss factor peak. It can be proved that, if $G_\infty/G_0 \to 1$, then the half-width of the loss factor peak approaches that of the loss modulus peak. Furthermore, both half-widths are identical if $\alpha = 1$ (conventional Zener model), and then the width for the loss factor peak is the smallest which is independent of the modulus dispersion:

$$W_\eta(\alpha = 1) = [W_\eta]_{min} = [W_l]_{min} = \log\frac{2+\sqrt{3}}{2-\sqrt{3}} = 1{\cdot}14. \tag{19}$$

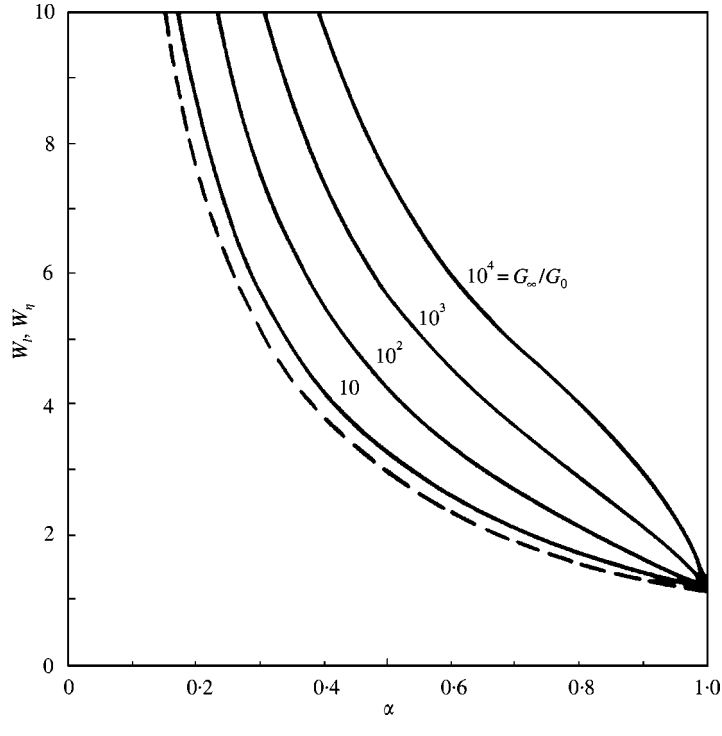

Figure 5. The half-width of the loss modulus (- - -) and loss factor (—) peak plotted against the value of α.

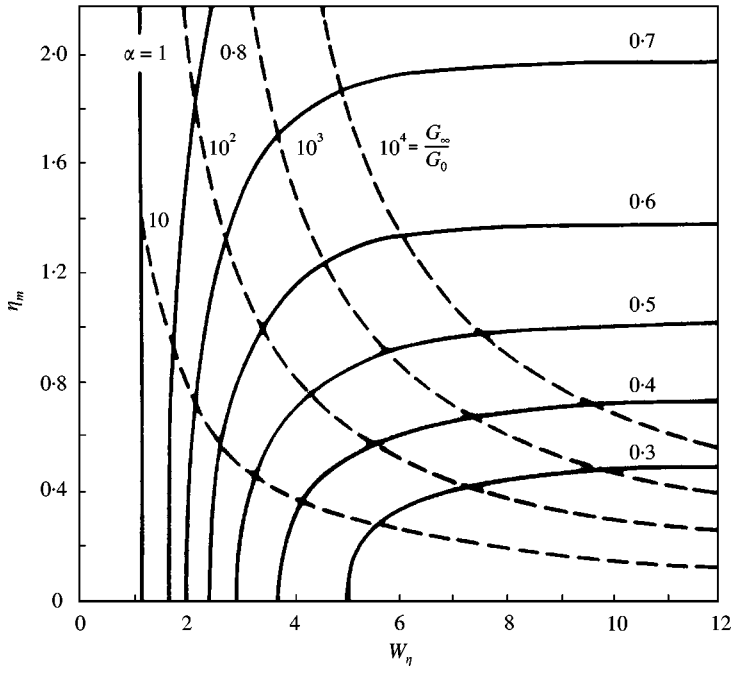

Figure 6. The fractional Zener model predicts that either proportionality or inverse proportionality may exist between the maximum and half-width of the loss factor peak.

It can be seen from equations (14) and (16) that both the maximum and width of the loss factor peak depend on both G_∞/G_0 and α. It follows that the maximum and width of the loss factor peak are interrelated through G_∞/G_0 and α. The conjugate values of η_m and W_η have been calculated for a number of values of G_∞/G_0 and α, and the results are shown in Figure 6 with dashed lines ($G_\infty/G_0 = 10, 10^2, 10^3, 10^4$; α varies) and solid lines ($\alpha = 0{\cdot}3$–$0{\cdot}8$; G_∞/G_0 varies). For the sake of completeness, the vertical line representing the conventional Zener model ($\alpha = 1{\cdot}0$, $W_\eta = 1{\cdot}14$) is also shown.

Figure 6 clearly demonstrates that the maximum and the half-width of the loss factor peak are inversely related to each other if one regards G_∞/G_0 as a parameter, and α as a variable (dashed line). This is in agreement with the prediction of Hartmann, who was the first to prove the inverse relation also by means of the fractional Zener model, referred to in his work as the Cole–Cole model [13]. The frequency curves of Figure 3 relate to this case. In contrast to this, Figure 6 shows that the inverse relation does not hold true if α is regarded as a parameter and G_∞/G_0 as a variable (solid line). In this case, the loss factor increases at the same time as the peak broadens, as seen in Figure 4.

To sum up, the fractional Zener model does not predict an unequivocal relation between the loss factor maximum and width, but proves that either proportionality or inverse proportionality may exist. Therefore, the inverse relation of the maximum to width of the loss factor peak, according to the fractional Zener model, cannot be regarded as a law which would be generally valid for polymers and other viscoelastic materials, although it may hold true for some of them.

It should finally be noted that the application of the fractional Zener model is limited to the symmetrical loss peak. However, asymmetrical peaks are often experienced for polymeric materials. Asymmetrical loss peaks can effectively be described by the

Havriliak–Negami model, the complex modulus for which is [23]

$$\frac{\bar{G}(\mathrm{j}\omega) - G_\infty}{G_0 - G_\infty} = \frac{1}{[1 + (\mathrm{j}\omega\tau_r)^\alpha]^\beta}. \tag{20}$$

where the value of exponent β serves to "tune" the peak asymmetry; $0 < \beta \leqslant 1$. This model is an empirical one, and can formally be considered as a modification of the fractional Zener model. This fact is clear from a comparison of equations (6b) and (20). The relation between the magnitude and width of the loss factor peak for the Havriliak–Negami model was investigated in the work of Hartmann *et al.* [14]. The authors determined the conjugate values of the loss factor and half-width by varying the exponent α for fixed values of G_∞/G_0 and β, and the inverse relation between η_m and W_η was found. Notwithstanding this, the comparison of equations (6b) and (20) suggests that the inverse relation also does not hold true for the Havriliak–Negami model, if the exponents α and β are regarded as constants, and the G_∞/G_0 modulus dispersion is varied. It follows that the predictions of the fractional Zener model also quantitatively hold true for the case of an asymmetrical loss peak.

2.3. VERIFICATION BY DISPERSION RELATIONS

All the conclusions discussed above have been drawn from the behaviour of the fractional Zener model. Consequently, these conclusions are as valid, general and accurate as the model itself. The fractional Zener model has evolved empirically, but today it is well-known that the model has a sound theoretical basis. The model relies on the constitutive equation of differential operator form of linear viscoelastic behaviour of solid materials [18, 20], and satisfies the thermodynamic constraints [19]. The model is universal in the sense that it does not imply any restriction, with the exception of linearity, on the mechanism of damping, and, therefore, the model may be applicable to materials of different kinds. The suitability of the fractional Zener model has indeed been proved for a wide variety of materials, including geological strata [17], glasses [17, 20], metals [17], and especially for polymeric damping materials [16, 18–20]. All these suggest that the model predictions are of a general nature and may be related, in principle, to the loss factor peak of any solid material regardless of damping mechanism.

In spite of the above, the fractional Zener model is no more than a model, and its applicability has limits. Naturally, the validity of model predictions depends on that of the model itself. Nevertheless, it can be proved that the model predictions for the relations between magnitude and width of the loss factor peak are in agreement with some fundamental physical principles, and, therefore, the validity of these relations is beyond the limits of the fractional Zener model. Such a fundamental principle is that of causality, which has led to the formulation of the universal Kramers–Kronig dispersion relations. The relations applied to the complex modulus of elasticity link the frequency dependence of the dynamic modulus to that of the loss properties. One form of the dispersion relations for the complex shear modulus is [1]

$$G_d(\omega) = G_0 - \frac{2\omega^2}{\pi} \int_0^\infty \frac{G_l(u)/u}{u^2 - \omega^2}\, \mathrm{d}u, \tag{21}$$

$$G_l(\omega) = \frac{2\omega}{\pi} \int_0^\infty \frac{G_d(u)}{u^2 - \omega^2}\, \mathrm{d}u, \tag{22}$$

where u is an integration variable. These relations are completely general and valid for any solid material, since the causal behaviour is an inevitable feature of real solids.

The simplified, approximate version of these relations which is useful for the present purpose, is [1]

$$\eta(\omega) \approx \frac{\pi}{2} \frac{\mathrm{d}[\log G_d(\omega)]}{\mathrm{d}[\log \omega]}. \tag{23}$$

This equation relates the loss factor at one frequency to the slope of the frequency variation of dynamic modulus plotted in a log–log co-ordinate system at that frequency. Recently, it has been proved that equation (23) always properly reflects the qualitative relation between these quantities [21]. Moreover, it has been proved that the accuracy of this approximate equation is better than 10%, if the slope of $\log \eta$ versus $\log \omega$ is smaller than 0·35 [21]. Consequently, equation (23) can be used not only for qualitative, but also for quantitative investigations, with some caution.

Equation (23) shows that the higher the loss factor, the larger the slope of frequency increase of dynamic modulus in a log–log co-ordinate system. It follows that the loss factor peak maximum occurs at around the inflexion point of the $\log G_d(\omega)$ versus $\log \omega$ curve, as seen in Figure 7. That is

$$\eta_m \approx \frac{\pi}{2} \left. \frac{\mathrm{d}[\log G_d(\omega)}{\mathrm{d}[\log \omega]} \right|_{max} \approx \frac{\pi}{2} s_{max}. \tag{24}$$

Moreover, Figure 7 demonstrates that the ω_1 lower and ω_2 upper limiting frequencies of the half-width of the loss peak occur near the location of the half-slope of $\log G_d(\omega)$ versus $\log \omega$ curve. That is

$$\frac{\eta_m}{2} \approx \frac{\pi}{4} s_{max} \approx \frac{\pi}{2} \frac{\mathrm{d}[\log G_d(\omega_1)]}{\mathrm{d}[\log \omega_1]} \approx \frac{\pi}{2} \frac{\mathrm{d}[\log G_d(\omega_2)]}{\mathrm{d}[\log \omega_2]} \tag{25}$$

provided that $\alpha < 0{\cdot}35$. The accuracy of this approximate equation decreases with increasing α, but the half-width is always proportional to the difference of frequencies at the half-slope of dynamic modulus–frequency curve.

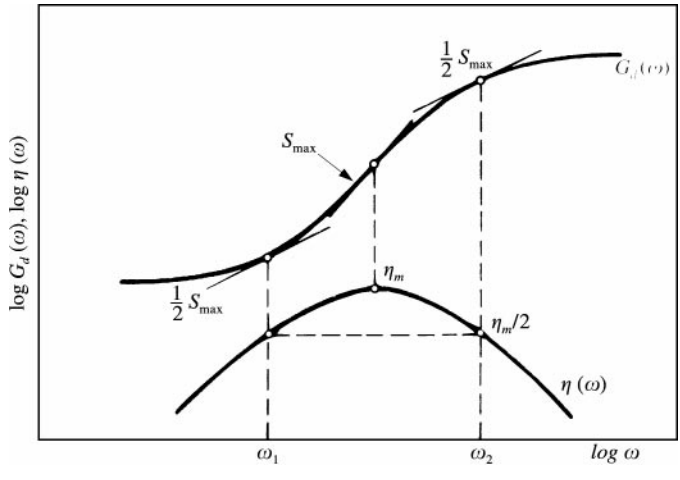

Figure 7. The magnitude and half-width of the loss factor peak are related to the s slope of $\log G_d$ versus $\log \omega$ curve. (It has been assumed in drawing the figure that α is smaller than 0·35.)

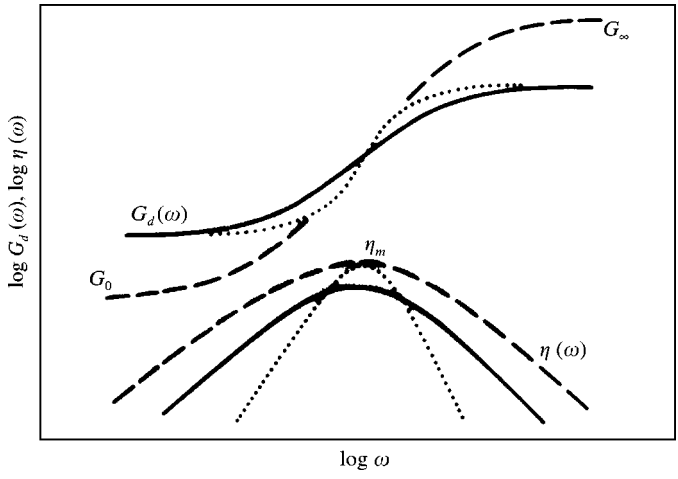

Figure 8. The width of the loss factor peak may either decrease or increase at the same time with the increase of peak maximum according to the dispersion relations.

Now assume that the loss factor is somehow increased. Figure 8 demonstrates the increase of the loss factor maximum and the related phenomena for two cases. It is clear from the foregoing that the increase of the loss factor in each case is accompanied by an increase of slope of the dynamic modulus–frequency curve. First, it is assumed that the modulus dispersion G_∞/G_0 remains unchanged while the loss factor is increased (dotted line). Then the half-width of the loss peak must be decreased to satisfy equation (23). Consequently, an inverse relation can be observed between the magnitude and width of the loss factor peak in this case. In contrast to this, if the modulus dispersion G_∞/G_0 can be increased at the same time as the loss factor maximum increases, then the peak will broaden (dashed line). This latter case is in agreement with the prediction of the fractional Zener model that the loss factor may increase while simultaneously the peak broadens. Consequently, the dispersion relations qualitatively verify that either a direct or an inverse relation may exist between the maximum and width of the loss factor peak. Bearing in mind the universal validity of the dispersion relations, it can be stated that the predictions of the fractional Zener model qualitatively hold true for the loss factor peak of any real solid material regardless of the actual damping mechanism.

3. EXPERIMENTAL EVIDENCE

Most experimental data on dynamic properties, covering a wide frequency range, are available for polymers, mainly elastomers used for sound and vibration damping. These are materials for which an inverse relation between the magnitude and width of the loss factor peak has been found. Therefore, the elastomers are the focus of this paper to verify the predictions of the fractional Zener model by experimental data, with special respect to the validity of the inverse relation. In addition, experimental data on some rigid plastics are presented and evaluated for the sake of completeness and interest.

A number of published experimental results were reviewed, studied and evaluated carefully by the author in order to find reliable data for the verification process. The loss factor peak was the centre of interest and, therefore, a material was selected only if the experimental data covered a sufficiently wide frequency range, and exhibited low scatter so

that the peak magnitude and the half-width could unambiguously be determined from the data. Surprisingly, it was noticed that finding such data, in spite of the numerous measurement results, is not a simple task. Additionally, an effort was made to find a symmetrical loss factor peak, but some asymmetry was always present. Moreover, neither the slope of frequency variation of the loss factor, measured far from the peak maximum, nor the low and high frequency limit values of dynamic modulus could reliably be determined even when the experimental data covered several decades of frequency.

In view of the above-mentioned difficulties, it was decided not to verify quantitatively the model prediction that the η_m loss factor maximum and the W_η half-width are interrelated through the G_∞/G_0 modulus dispersion and the α slope of frequency variation of the loss factor. It is not worth making great efforts to quantitatively verify this interrelation, because the accuracy and applicability of the fractional Zener model, like any others, evidently have limits. Nor was it aimed at fitting the experimental data to the fractional Zener model and using the model parameters so determined for the verification, because it is not correct methodologically. Instead, it was aimed at verifying quantitatively only the relation between η_m and W_η predicted by the model using those values which were read off from the available experimental loss factor peaks after careful consideration and evaluation. It is believed that this method is not only simple, but much more reliable than any other, to find the relation between η_m and W_η, and, therefore, it enables the model predictions to be verified at least qualitatively.

The loss factor maximum and half-width determined for ten elastomers, which are used or applicable for vibration damping, are given in Table 1. The materials include three polyurethane samples [8], the damping materials GE. SMRD [24] and EAR C-1002 [25], two acrylic adhesives (3M ISD-112 [26] and 3M-467 [27]) used as damping tapes, a polyisobutylene [28] and two urethane–epoxy interpenetrating network (IPN) polymers [12] developed also for damping purposes. These data concern the loss properties in shear or elongation deformation, which are nearly identical for elastomers. Note that all experimental loss factor peaks used for the determination of η_m and W_η have been constructed by applying the temperature–frequency equivalence principle. The reference temperatures are given in Table 1. The loss factor peaks, with the exception of the polyurethane samples, occur in the audio frequency range or close to it.

The relations between the experimental values of η_m and W_η are seen in Figure 9, where the appropriate theoretical curves calculated by the fractional Zener model are also drawn for the sake of orientation. It is easy to recognize either the proportionality, or the inverse

TABLE 1

The experimental values of maximum and half-width of the loss factor peak determined for elastomeric damping materials

Material	T(°C)	η_m	W_η	Reference
Polyurethane (a)	25	1·0	4·0	8, p. 1848
Polyurethane (b)	25	0·67	5·55	8, p. 1849
Polyurethane (c)	25	0·38	10·4	8, p. 1849
Damping material, GE.SMRD		0·9	3·3	24, p. 15
Damping material, EAR C-1002	10	1·12	3·85	25, p. 15
Acrylic adhesive, 3M ISD-112		1·19	4·26	26
Acrylic adhesive, 3M-467	24	1·28	5·22	27
Polyisobutylene	20	1·4	4·2	28
Urethane–epoxy IPN (a)	10	1·6	3·74	12, p. 378
Urethane–epoxy IPN (b)	10	2·1	3·92	12, p. 380

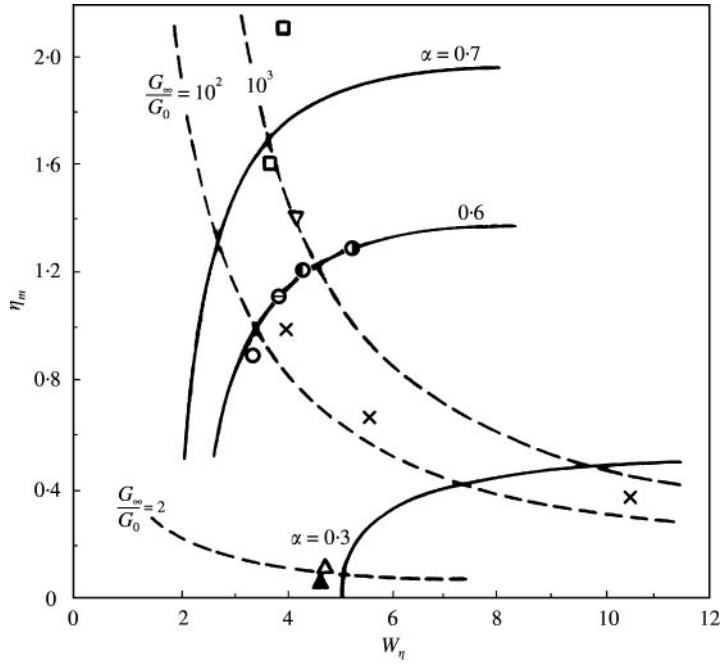

Figure 9. The experimental values of maximum and half-width of the loss factor peak determined for polymeric materials. Elastomers: +, polyurethanes; ○, GE.SMRD; ⊖, EAR C-1002; ◐, acrylic adhesive, 3M ISD-112, ◑, acrylic adhesive, 3M-467; ▽, polyisobuthylene; □, urethane–epoxy IPN polymers. Rigid plastics; △, PVC; ▲, polymethylmethacrylate; —,---, prediction of the fractional Zener model.

proportionality between the loss factor maxima and half-widths. The inverse proportionality is observable if the polyurethanes and the damping material EAR C-1002 are considered. In contrast to this, if the damping materials GE.SMRD, EAR C-1002, the polyurethane sample (a) and the two acrylic adhesives are considered, then the proportionality is evident. These data convincingly demonstrate that the higher the loss factor, the broader the peak, which is in contradiction to the common belief in an inverse relation between η_m and W_η. Moreover, if the polyurethane sample (a), the damping material EAR C-1002, the polyisobutylene and the two IPN polymers are compared, it can be seen that the half-widths are about the same ($W_\eta \approx 4$), while the loss factors of these materials are dissimilar; with η_m ranging from 1·0 to 2·1, this again contradicts the inverse relation. Consequently, the experimental data presented in Figure 9 qualitatively support the prediction of the fractional Zener model that the relation between the magnitude and width of the loss factor peak is not unequivocal; either the proportionality or the inverse proportionality may exist between them. The experimental data definitely disprove the idea that the inverse relation would be a law which is generally valid for elastomeric materials.

Although the interrelation between η_m and W_η through G_∞/G_0 and α has not been verified quantitatively, it is instructive to make an estimation of the maximum and half-width of the loss factor peak of elastomeric materials by means of equations (14) and (16) respectively. The estimation can be performed since the values of G_∞/G_0 and α are quite well known from numerous measurements performed on elastomers. Specifically, it has been found that the most typical values of G_∞/G_0 of elastomeric materials occur between 10^2 and 10^3, and the relevant α slope ranges from about 0·5 to 0·7 [14, 19]. Using these parameters, the calculations by equations (14) and (16) result in the loss factor maxima and the half-widths

TABLE 2

The experimental values of maximum and half-width of the loss factor peak determined for two rigid plastics

Material	T(°C)	η_m	W_η	Reference
PVC (unplasticized)	21	0·048	4·6	2, p. 189
Polymethylmethacrylate (Plexiglas M 33)	24	0·1	4·7	29

are $0{\cdot}8 < \eta_m < 1{\cdot}8$, and $2{\cdot}5 < W_\eta < 6$ respectively. These values are in good accord with those seen in Figure 9, which are quite typical for elastomeric damping materials [14].

Of the polymers and other solid materials known so far, the elastomers have the highest damping. The high loss factor of elastomeric materials is due to the intensive rubber to glass transition phenomenon associated with large modulus dispersion. It has been mentioned in section 2.1 that the existence of at least one loss peak and the corresponding modulus dispersion are characteristics of any solid material. The loss peak and the modulus dispersion are always related to a transition of some kind. The loss peak is also observable in rigid plastics which are polymers in a glassy state. The maximum and half-width of the loss factor peak determined by the method described above for two rigid plastics (an unplasticized PVC [2] and polymethylmethacrylate, also known as Plexiglas [29]), are given in Table 2 and presented in Figure 9 for the sake of interest. The loss peak of these materials is a consequence of the so-called secondary transition occurring in glassy state of organic polymers. It is known that the secondary transition is associated with weak dispersion of dynamic modulus ($G_\infty/G_0 \approx 2$–3 [2]) and, therefore, the loss factor is low. Nevertheless, the peak is broad, which is mainly explained by the weak frequency variation of the loss factor characterizing the rigid plastics; the relevant α slope is around 0·2–0·3 or even smaller [2]. The appropriate theoretical curves calculated by the fractional Zener model ($G_\infty/G_0 = 2$ and $\alpha = 0{\cdot}3$) are drawn in Figure 9. It can be seen that both the magnitude and half-width of the loss factor peak, and their interrelation, are in quite good accord with the model predictions for these materials also.

4. CONCLUSIONS

The relation between the magnitude and width of the loss factor peak of viscoelastic materials has been investigated in this paper by means of the fractional derivative Zener model, with special reference to polymeric damping materials. As a result of theoretical investigation, the following main conclusions can be drawn.

(1) The magnitude and the width of the loss factor peak are interrelated through the dispersion of dynamic modulus and the rate of frequency variation of the loss factor measured far from the peak.
(2) Either proportionality or inverse proportionality may exist between the magnitude and width of the loss factor peak. This conclusion disproves the belief that the inverse relation would be a generally valid law for polymeric materials.
(3) According to the model predictions, there is no fundamental barrier to increasing the loss factor while simultaneously broadening the peak width. Therefore, the way is open, from a theoretical point of view, to develop highly efficient damping materials having high loss over a broad frequency range.

All the above conclusions have been drawn from the behaviour of the fractional derivative Zener model, for which the loss factor peak is symmetrical with respect to logarithmic frequency. Nevertheless, it has been shown that the predictions of this model also hold qualitatively true for asymmetrical peaks. Moreover, it has been verified by means of the Kramers–Kronig dispersion relations that the validity of theoretical predictions is beyond the limits of the model, and qualitatively are valid for the loss factor peak of any solid material regardless of the actual mechanism of damping. The experimental data presented support the theoretical conclusions.

ACKNOWLEDGMENTS

This work is a part of a research project supported by the Hungarian Research Fund (OTKA) under contract T 30151. The financial support is gratefully acknowledged.

REFERENCES

1. N. W. TSCHOGEL 1989 *The Phenomenological Theory of Linear Viscoelastic Behaviour*: *An Introduction*. Berlin: Springer.
2. B. E. READ and G. D. DEAN 1978 *The Determination of Dynamic Properties of Polymers and Composites*. Bristol, UK: Adam Hilger.
3. J. D. FERRY 1980 *Viscoelastic Properties of Polymers*. New York: Wiley; third edition.
4. A. D. NASHIF, D. I. G. JONES and J. P. HENDERSON 1985 *Vibration Damping*. New York: Wiley.
5. T. PRITZ 1998 *Journal of Sound and Vibration* **214**, 83–104. Frequency dependences of complex moduli and complex Poisson's ratio of real solid materials.
6. A. R. PAYNE and J. R. SCOTT 1960 *Engineering Design with Rubber*. London: Maclaren, 34.
7. R. N. CAPPS and L. L. BEUMEL 1990 *Sound and Vibration Damping with Polymers*, *ACS Symposium Series* 424 (R. D. Corsaro and L. H. Sperling, editors), 63–78. Washington, DC: American Chemical Society. Application of polymer development to constrained-layer damping.
8. B. HARTMANN, J. V. DUFFY, G. F. LEE and E. BALIZER 1988 *Journal of Applied Polymer Science* **35**, 1829–1852. Thermal and dynamic mechanical properties of polyurethaneureas.
9. J. V. DUFFY, G. F. LEE, J. D. LEE and B. HARTMANN 1990 *Sound and Vibration Damping with Polymers*, *ACS Symposium Series* 424 (R. D. Corsaro and L. H. Sperling, editors), 281–300. Washington, DC: American Chemical Society. Dynamic mechanical properties of poly(tetramethylene ether) glycol polyurethanes.
10. G. F . LEE, J. D. LEE, B. HARTMANN and D. RATHNAMMA 1993 *Proceedings of Damping* '93, *San Francisco*, Vol. 3, ICA 1–19. Damping properties of PTMG/PPG blends.
11. N. CAPPS 1986 *Rubber Chemistry and Technology* **59**, 103–122. Effect of cure systems and reinforcing fillers on dynamic mechanical properties of chlore-butyl elastomers for potential vibration-control applications.
12. R. Y. TING, R. N. CAPPS and D. KLEMPNER 1990 *Sound and Vibration Damping with Polymers*, *ACS Symposium Series* 424 (R. D. Corsaro and L. H. Sperling, editors), 366–381. Washington, DC: American Chemical Society. Acoustical properties of some interpenetrating network polymers. Urethane-epoxy networks.
13. B. HARTMANN 1990 *Sound and Vibration Damping with Polymers*, *ACS Symposium Series* 424 (R. D. Corsaro and L. H. Sperling, editors), 23–45. Washington, DC: American Chemical Society. Relation of polymer chemical composition to acoustic damping.
14. B. HARTMANN, G. F. LEE and J. D. LEE 1994 *Journal of the Acoustical Society of America* **95**, 226–233. Loss factor height and width limits for polymer relaxations.
15. F. MAINARDI 1994 *Journal of Alloys and Compounds* **211/212**, 534–538. Fractional relaxation in anelastic solids.
16. T. PRITZ 1996 *Journal of Sound and Vibration* **195**, 103–115. Analysis of four-parameter fractional derivative model of real solid materials.
17. M. CAPUTO and F. MAINARDI 1971 *Pure and Applied Geophysics* **91**, 134–147. A new dissipation model based on memory mechanism.

18. L. ROGERS 1983 *Journal of Rheology* **27**, 351–372. Operators and fractional derivatives for viscoelastic constitutive equations.
19. R. L. BAGLEY and P. J. TORVIK 1986 *Journal of Rheology* **30**, 133–135. On fractional calculus model of viscoelastic behaviour.
20. P. J. TORVIK and R. L. BAGLEY 1987 *The Role of Damping in Vibration and Noise Control* (L. Rogers and J. C. Simonis, editors), DE-Vol. 5, 125–135. New York: ASME. Fractional derivatives in the description of damping materials and phenomena.
21. T. PRITZ 1999 *Journal of Sound and Vibration* **228**, 1145–1165. Verification of local Kramers–Kronig relations for complex modulus by means of fractional derivative model.
22. K. S. COLE and R. H. COLE 1941 *Journal of Chemical Physics* **9**, 341–351. Dispersion and absorption in dielectrics. I. Alternating current characteristics.
23. S. HAVRILIAK and S. NEGAMI 1967 *Polymer* **8**, 161–210. A complex plane representation of dielectric and mechanical relaxation processes in some polymers.
24. C. CHESNEAU, J. Y. CAVAILLE and J. P. LAURES 1989 *Proceedings of Damping* '89, *FL*, Vol. 2, FAD 1–22. Complex modulus measurements over a wide range of frequencies and material characteristics through the confrontation of two instruments.
25. D. I. G. JONES 1991 *Proceedings of Damping* '91, *San Diego*, *CA*, Vol. 2, EBD 1–18. Results of a Round Robin test series to evaluate complex moduli of a selected damping material.
26. B. R. ALLEN and E. D. PINSON 1991 *Proceedings of Damping* '91, *San Diego*, *CA*, Vol. 2, EAE 1–14. Complex stiffness test data for three viscoelastic materials by the direct complex stiffness method.
27. D. I. G. JONES and M. L. PARIN 1972 *Journal of Sound and Vibration* **24**, 201–210. Technique for measuring damping properties of thin viscoelastic layers.
28. D. I. G. JONES 1980 *Damping Applications for Vibration Control* (P. J. Torvik, editor), 27–51. New York: ASME. Viscoelastic materials for damping applications.
29. J. KOPPELMANN 1958 *Rheologica Acta* **1**, 20–28. Über die Bestimmung des dynamischen Elastizitätsmoduls und des dynamischen Schubmoduls im Frequenzbereich von 10^{-5} bis 10^{-1} Hz.